

Convergence to a self-similar solution in general relativistic gravitational collapse

Tomohiro Harada* and Hideki Maeda†

Department of Physics, Waseda University, Shinjuku, Tokyo 169-8555, Japan

(Received 14 November 2000; published 27 March 2001)

We study the spherical collapse of a perfect fluid with an equation of state $P=k\rho$ by full general relativistic numerical simulations. For $0 < k \leq 0.036$, it has been known that there exists a general relativistic counterpart of the Larson-Penston self-similar Newtonian solution. The numerical simulations strongly suggest that, in the neighborhood of the center, generic collapse converges to this solution in an approach to a singularity and that self-similar solutions other than this solution, including a “critical solution” in the black hole critical behavior, are relevant only when the parameters which parametrize initial data are fine-tuned. This result is supported by a mode analysis on the pertinent self-similar solutions. Since a naked singularity forms in the general relativistic Larson-Penston solution for $0 < k \leq 0.0105$, this will be the most serious known counterexample against cosmic censorship. It also provides strong evidence for the self-similarity hypothesis in general relativistic gravitational collapse. The direct consequence is that critical phenomena will be observed in the collapse of isothermal gas in Newton gravity, and the critical exponent γ will be given by $\gamma \approx 0.11$, though the order parameter cannot be the black hole mass.

DOI: 10.1103/PhysRevD.63.084022

PACS number(s): 04.20.Dw, 04.25.Dm, 04.40.Nr

I. INTRODUCTION

There is no characteristic scale in general relativity as well as in Newton gravity. A set of field equations is invariant by scale transformations if we assume appropriate matter fields. It implies the existence of scale-invariant solutions to the field equations. Such solutions are called self-similar solutions, which are defined by the existence of a homothetic Killing vector field. Although the self-similar solutions are only special solutions of Einstein equations, it often has been supposed that these solutions play an important role in situations where gravity is an essential ingredient in a spherically symmetric system (for example, Carr [1]). Such an assumption can be called the *self-similarity hypothesis*.

A spherically symmetric self-similar system of a perfect fluid has been widely researched. Self-similar solutions in Newton gravity have been researched in an effort to obtain simple and realistic solutions of gravitational collapse [2–5]. In particular, the Larson-Penston solution, which is one of the self-similar solutions, is believed to describe the central part of generic spherical collapse of isothermal gas. Recent numerical simulations and results of mode analyses strongly support this proposition [6–9]. In general relativity, a spherically symmetric self-similar system was discussed in various situations, such as cosmological voids, gravitational collapse, primordial black holes [10–12], and so on. The detailed structure of self-similar collapse solutions were analyzed [13]. The discovery of the black hole critical behavior shed light on the importance of a self-similar solution as a critical solution [14,15]. Several very recent works have been done in complete classification of self-similar solutions [16–20].

In the context of the black hole critical behavior, the self-similar critical solution is not an attractor. A renormalization group approach showed that the critical solution has only one

repulsive mode [21,22]. The critical exponent which appears in the scaling law of the formed black hole mass is equal to the inverse of the eigenvalue of the repulsive mode for a perfect fluid case.

In the context of cosmic censorship [23,24], a spherical system of a pressureless fluid (dust) has been extensively examined since it can be solved exactly. It has been shown that a naked singularity forms in generic spherical collapse of dust from an analytic initial density profile [25,26]. It is noted that this solution is not self-similar at all. In the presence of pressure, self-similar solutions were investigated by Ori and Piran [13,27,28]. For an adiabatic equation of state $P=k\rho$ ($0 < k \leq 0.4$), they found a discrete set of self-similar solutions which are analytic both at the center and at the sonic point. They discovered the general relativistic counterpart of the Larson-Penston solution for $0 < k \leq 0.036$. They observed that a naked singularity forms in this solution for $0 < k \leq 0.0105$. They also observed that there exist analytic self-similar solutions with naked singularity for every k . Harada [29] showed the generic occurrence of naked singularity in spherical collapse of a perfect fluid for $0 < k \leq 0.01$ by numerical simulations using the code based on the Hernandez-Misner formulation without the ansatz of self-similarity.

The aim of this paper is to examine the validity of the self-similarity hypothesis for a spherical system of a perfect fluid and to understand the relation of the self-similarity hypothesis, critical behavior and cosmic censorship. In this paper, we adopt the geometrized unit.

II. BASIC EQUATIONS

A. Einstein equation

We adopt the comoving coordinates. The line element in a spherically symmetric spacetime is given by

$$ds^2 = -e^{\sigma(t,r)} dt^2 + e^{\omega(t,r)} dr^2 + R^2(t,r)(d\theta^2 + \sin^2\theta d\phi^2). \quad (2.1)$$

*Email address: harada@gravity.phys.waseda.ac.jp

†Email address: hideki@gravity.phys.waseda.ac.jp

It is noted that the comoving coordinates may be able to cover even inside of the apparent horizon. We consider a perfect fluid

$$T^{\mu\nu} = (\rho + P)u^\mu u^\nu + P g^{\mu\nu}. \quad (2.2)$$

Then the Einstein equations and the equations of motion for the matter are reduced to the following simple form:

$$\frac{\partial m}{\partial r} = 4\pi R^2 \rho \frac{\partial R}{\partial r}, \quad (2.3)$$

$$\frac{\partial m}{\partial t} = -4\pi R^2 P \frac{\partial R}{\partial t}, \quad (2.4)$$

$$\frac{\partial \sigma}{\partial r} = -\frac{2}{\rho + P} \frac{\partial P}{\partial r}, \quad (2.5)$$

$$\frac{\partial \omega}{\partial t} = -\frac{2}{\rho + P} \frac{\partial \rho}{\partial t} - \frac{4}{R} \frac{\partial R}{\partial t}, \quad (2.6)$$

$$m = \frac{R}{2} \left[1 + e^{-\sigma} \left(\frac{\partial R}{\partial t} \right)^2 - e^{-\omega} \left(\frac{\partial R}{\partial r} \right)^2 \right], \quad (2.7)$$

where $m(t, r)$ is called the Misner-Sharp mass. We assume the following equation of state:

$$P = k\rho, \quad (2.8)$$

where we assume that $0 < k < 1$. For a barotropic equation of state, the existence of self-similar solution demands the above form. Moreover, this equation of state will be valid for isothermal gas in Newton limit and for relativistically high-density polytropes [13]. We define the following dimensionless functions [12]:

$$\eta \equiv 8\pi r^2 \rho, \quad (2.9)$$

$$S \equiv \frac{R}{r}, \quad (2.10)$$

$$M \equiv \frac{2m}{r}. \quad (2.11)$$

We also define the following zooming coordinates:

$$\tau \equiv -\ln(-t), \quad (2.12)$$

$$z \equiv \frac{r}{-t}. \quad (2.13)$$

It is found that Eqs. (2.5) and (2.6) can be integrated as

$$e^\sigma = a_\sigma(t) z^{\frac{4k}{1+k}} \eta^{-\frac{2k}{1+k}}, \quad (2.14)$$

$$e^\omega = a_\omega(r) \eta^{-\frac{2}{1+k}} S^{-4}, \quad (2.15)$$

where $a_\sigma(t)$ and $a_\omega(r)$ are arbitrary functions. This integrability is the advantage of the comoving coordinates. These

arbitrary functions correspond to the freedom of rescaling the time and radial coordinates as $\tilde{t} = \tilde{t}(t)$ and $\tilde{r} = \tilde{r}(t)$. Hereafter, we restrict this gauge freedom by choosing $a_\sigma = \text{const}$ and $a_\omega = 1$.

Being transformed into the zooming coordinates, the field equations are reduced to

$$M + M' = \eta S^2 (S + S'), \quad (2.16)$$

$$\dot{M} + M' = -k \eta S^2 (\dot{S} + S'), \quad (2.17)$$

$$\begin{aligned} \frac{M}{S} &= 1 + a_\sigma^{-1} (\eta z^{-2})^{2k/(1+k)} z^2 (\dot{S} + S')^2 \\ &\quad - \eta^{\frac{2}{1+k}} S^4 (S + S')^2, \end{aligned} \quad (2.18)$$

where the derivatives are abbreviated as

$$\dot{} \equiv \frac{\partial}{\partial \tau}, \quad (2.19)$$

$$' \equiv \frac{\partial}{\partial \ln z}. \quad (2.20)$$

For later convenience, we define the quantity y which is one third of the ratio of the ‘‘average density’’ of the region interior to r to the local density at r , defined as

$$y \equiv \frac{M}{\eta S^3}. \quad (2.21)$$

If we consider the regular center, then it is found from Eq. (2.3) that

$$y = \frac{1}{3} \quad (2.22)$$

at the regular center $z = +0$. We can define two velocity functions V_z and V_R . The V_z is the velocity of the $z = \text{const}$ line relative to the fluid element, which is written as

$$V_z = -z e^{(\omega - \sigma)/2}, \quad (2.23)$$

while V_R is the velocity of the $R = \text{const}$ line relative to the fluid element, which is written as

$$V_R \equiv -e^{(\omega - \sigma)/2} \frac{\left(\frac{\partial R}{\partial t} \right)}{\left(\frac{\partial R}{\partial r} \right)} = V_z \frac{\dot{S} + S'}{S + S'}. \quad (2.24)$$

B. Self-similar solutions

For self-similar solutions, we assume that all dimensionless quantities depend only on z : i.e.,

$$\eta = \eta(z), \quad (2.25)$$

$$S = S(z), \quad (2.26)$$

$$M = M(z), \quad (2.27)$$

$$\sigma = \sigma(z), \quad (2.28)$$

$$\omega = \omega(z). \quad (2.29)$$

The field equations are reduced to the following form:

$$(\ln M)' = \frac{k}{1+k}(y^{-1} - 1), \quad (2.30)$$

$$(\ln S)' = -\frac{1}{1+k}(1-y), \quad (2.31)$$

$$(1-y)^2 V_z^2 - (k+y)^2 + (1+k)^2 \eta^{-2/(1+k)} S^{-6} \left(1 - \frac{M}{S}\right) = 0, \quad (2.32)$$

where V_z and V_R are written as

$$V_z \equiv -a_\sigma^{-1/2} z^{(1-k)/(1+k)} \eta^{-(1-k)/(1+k)} S^{-2} \quad (2.33)$$

and

$$V_R = -V_z \frac{1-y}{k+y}, \quad (2.34)$$

respectively. It is noted that, although the apparent form of these equations does not seem to be an autonomous system, the original system before we have performed explicit integrations is, of course, an autonomous system. We can find that the fluid velocity, with respect to $R = \text{const}$, vanishes only if $V_z = 0$ or $y = 1$. The above set of equations together with appropriate boundary conditions is enough to determine the unknown functions $M(z)$, $S(z)$ and $\eta(z)$. However, in addition to the above equations, the following dependent equation is used:

$$(\ln \eta)' = 2 - \frac{4y V_z^2 - (1+k)^2 S^{-4} \eta^{-(1-k)/(1+k)}}{2(V_z^2 - k)}. \quad (2.35)$$

Using the fact that $y = 1/3$ is satisfied at $z = +0$, from Eqs. (2.30)–(2.32), we find the behavior of the solution around the regular center $z = +0$ as

$$M = \frac{C_k}{3} (2D)^{k/(1+k)} z^{2k/(1+k)} [1 + O(z^{2(1+3k)/3(1+k)})], \quad (2.36)$$

$$S = C_k^{1/3} (2D)^{-1/3(1+k)} z^{-2/3(1+k)} \times [1 + O(z^{2(1+3k)/3(1+k)})], \quad (2.37)$$

$$\eta = 2D z^2 [1 + O(z^{2(1+3k)/3(1+k)})], \quad (2.38)$$

and

$$y = \frac{1}{3} [1 + O(z^{2(1+3k)/3(1+k)})], \quad (2.39)$$

where C_k is a constant determined by k as

$$C_k \equiv \frac{3(1+k)}{1+3k}, \quad (2.40)$$

and the parameter D is defined as

$$D \equiv \frac{1}{2} \lim_{z \rightarrow +0} z^{-2} \eta = 4\pi\rho(t,0)t^2. \quad (2.41)$$

Therefore, solutions that have regular centers are parametrized by only one parameter D . Now that we find

$$e^\sigma = a_\sigma (2D)^{-2k/(1+k)} \quad (2.42)$$

at the regular center, we let e^σ be unity at the regular center by choosing the constant a_σ as

$$a_\sigma = (2D)^{2k/(1+k)}. \quad (2.43)$$

This gauge fixing gives the physical meaning to the parameter D . Then the behavior of V_z around the regular center is written as

$$V_z = -C_k^{-2/3} (2D)^{-1/3(1+k)} z^{(1+3k)/3(1+k)} \times [1 + O(z^{2(1+3k)/3(1+k)})]. \quad (2.44)$$

The system of equations has an apparent singularity at a point $z = z_{\text{sp}}$ at which the relative velocity of $z = \text{const}$ world line with respect to the fluid element is equal to the sound speed, i.e.,

$$V_z^2 = k. \quad (2.45)$$

Such a point is called a sonic point. The regularity requires the following condition at the sonic point:

$$4yk - (1+k)^2 \eta^{-(1-k)/(1+k)} S^{-4} = 0. \quad (2.46)$$

Every regular solution must cross the sonic point, satisfying Eq. (2.46).

Ori and Piran [13] discovered the band structure of solutions regular both at the center and at the sonic point. In particular, there is only a discrete set of solutions which are analytic at the sonic point. Here, we give special attention to such solutions. One of such solutions is the flat Friedmann (FF) solution. There are another types of analytic solutions which are called the ‘‘black hole’’ type solutions, in which a massive singularity forms at $t = 0$ and after that the mass of the singularity grows linearly with t , and the ‘‘repulsive’’ type solutions, in which the central singularity which forms at $t = 0$ disappears instantaneously and the cloud begins to expand at $t = 0$. The solutions are characterized by the number of oscillations in the velocity field V_R .

Then we consider the behavior of the analytic similarity solutions. For the FF solution it is found that

$$D = \frac{2}{3} \frac{1}{(1+k)^2}. \quad (2.47)$$

The solution is written as

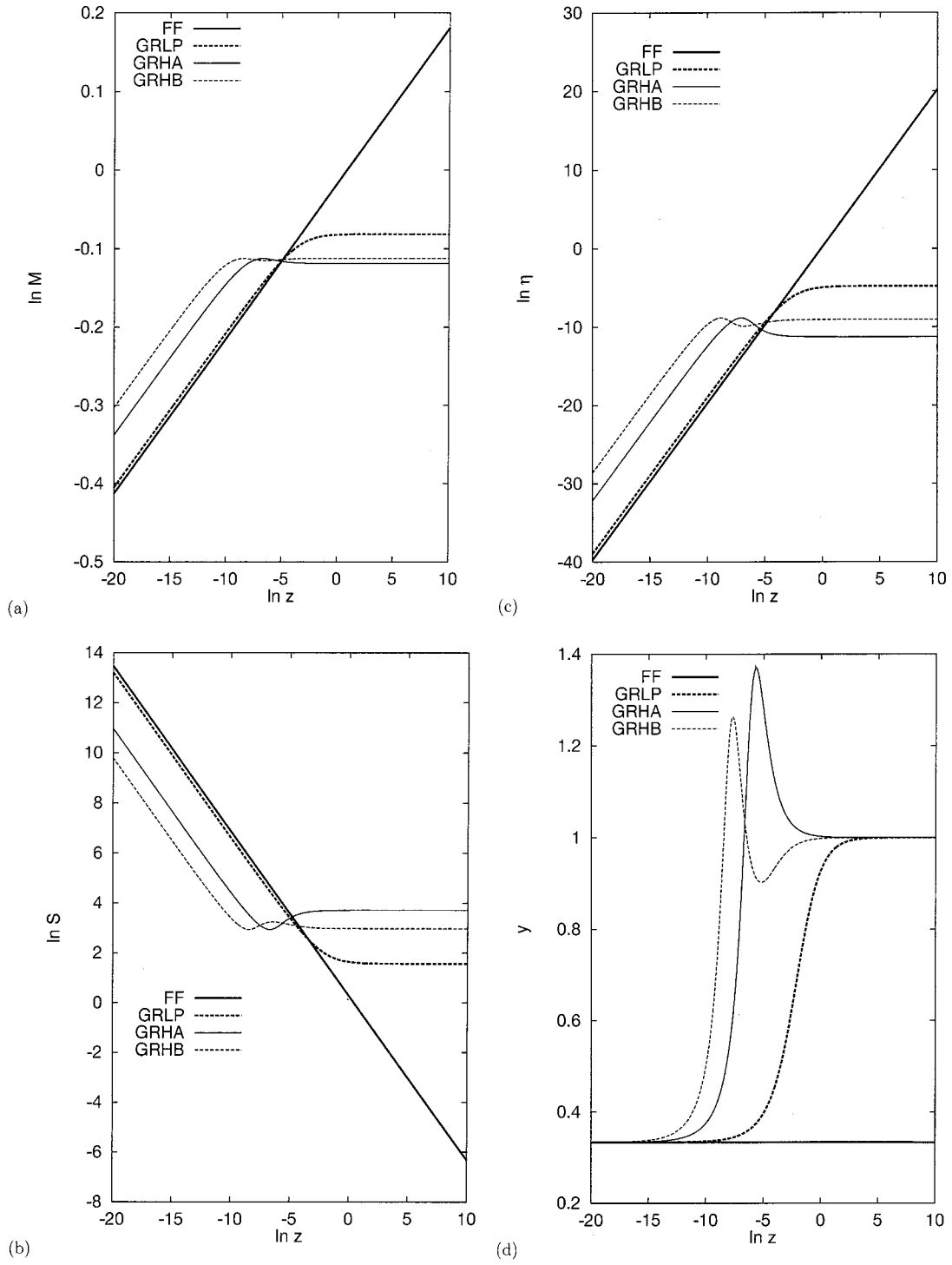


FIG. 1. Self-similar solutions for $k=0.01$. (a) $\ln M$, (b) $\ln S$, (c) $\ln \eta$, (d) y , (e) $-V_z$, and (f) $-V_R$ are plotted. In (g), the ordinate and abscissa are $4\pi\rho t^2$ and $R/(-t)$, respectively.

TABLE I. Values of D for self-similar solutions.

	$k=0.001$	0.008	0.01	0.03
FF	$2/(3 \times 1.001^2)$	$2/(3 \times 1.008^2)$	$2/(3 \times 1.01^2)$	$2/(3 \times 1.03^2)$
GRLP	1.640	1.480	1.439	1.119
GRHA	1.675×10^3	1.345×10^3	1.265×10^3	7.204×10^2
GRHB	7.170×10^4	4.903×10^4	4.414×10^4	1.650×10^4

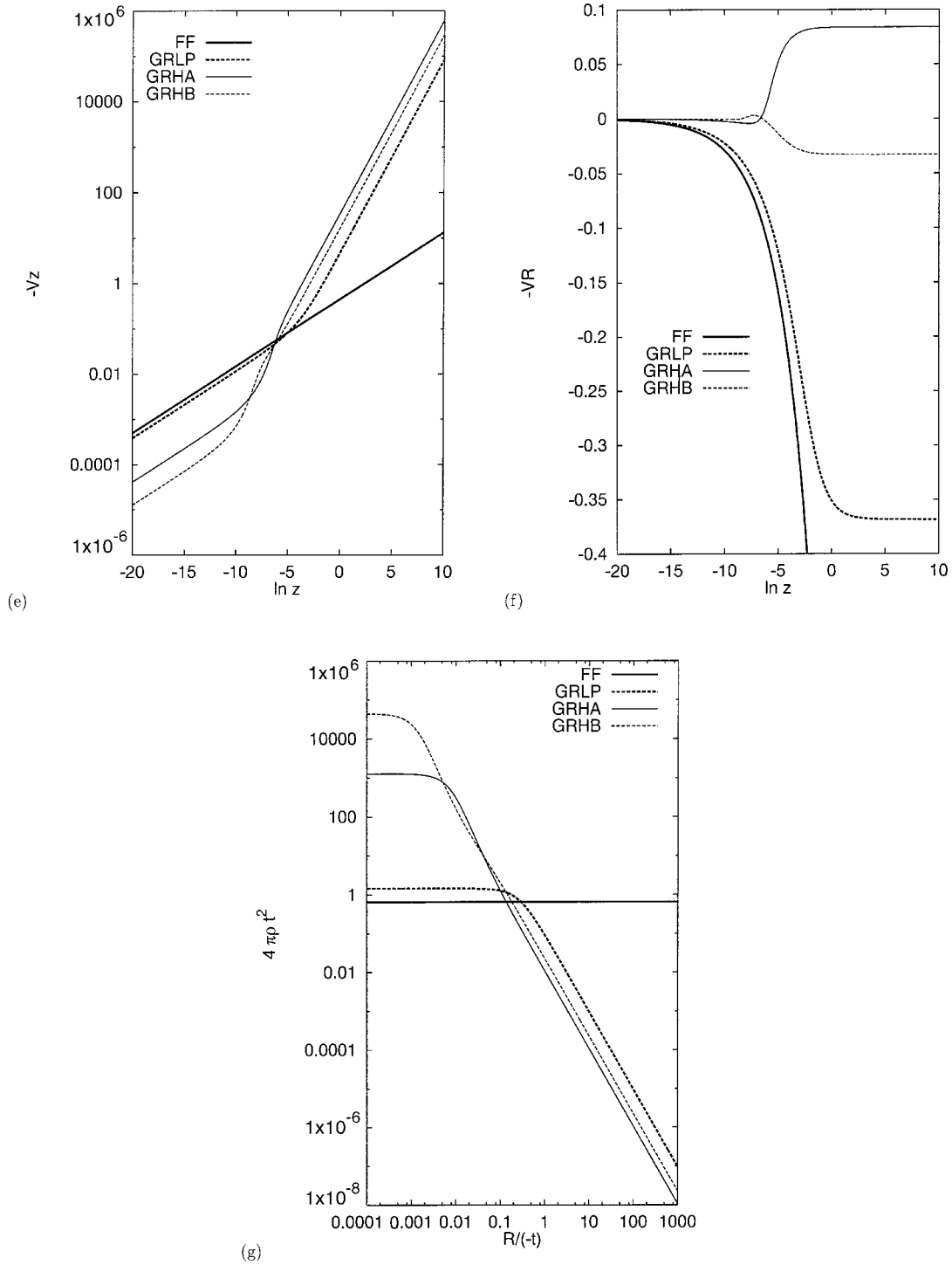


FIG. 1. (Continued.)

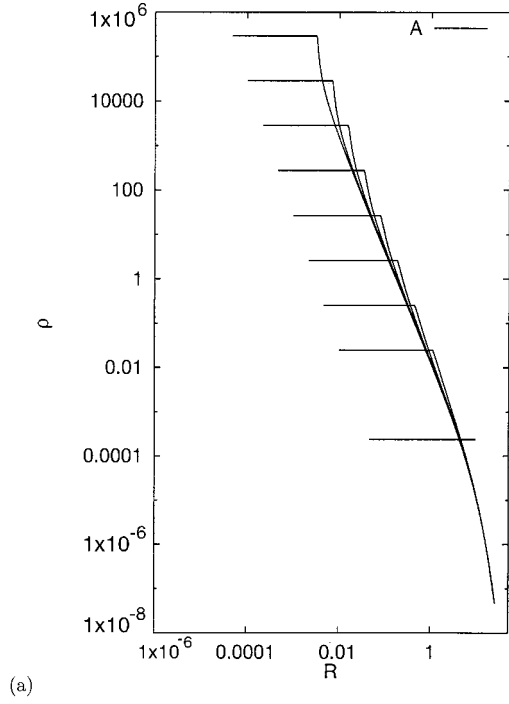
$$M = \frac{C_k}{3} \left(\frac{4}{3(1+k)^2} \right)^{k/(1+k)} z^{2k/(1+k)}, \quad (2.48)$$

$$S = C_k^{1/3} \left(\frac{4}{3(1+k)^2} \right)^{-1/3(1+k)} z^{-2/3(1+k)}, \quad (2.49)$$

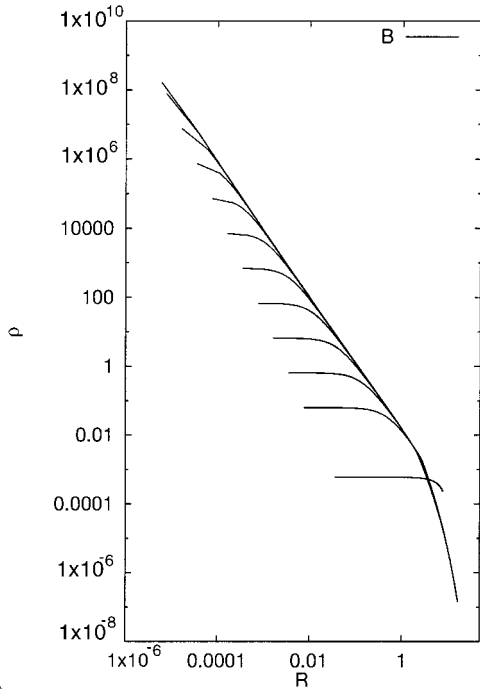
$$\eta = 2Dz^2, \quad (2.50)$$

TABLE II. Models for numerical simulations.

Models	Initial density profile	Initial compactness ($\mathcal{M}/R_{s,i}$)
A	Homogeneous	1/10
B	Inhomogeneous	1/10
C	Homogeneous	1/30
D	Inhomogeneous	1/30



(a)



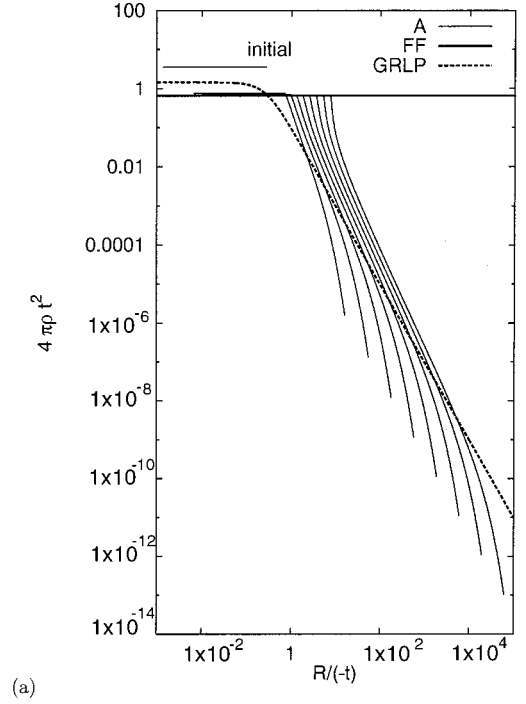
(b)

FIG. 2. Time evolution of the density profile as for models (a) A and (b) B for $k=0.01$ are plotted. The ordinate and abscissa are the density ρ and the circumferential radius R , respectively. The unit is chosen so that the ADM mass \mathcal{M} is unity.

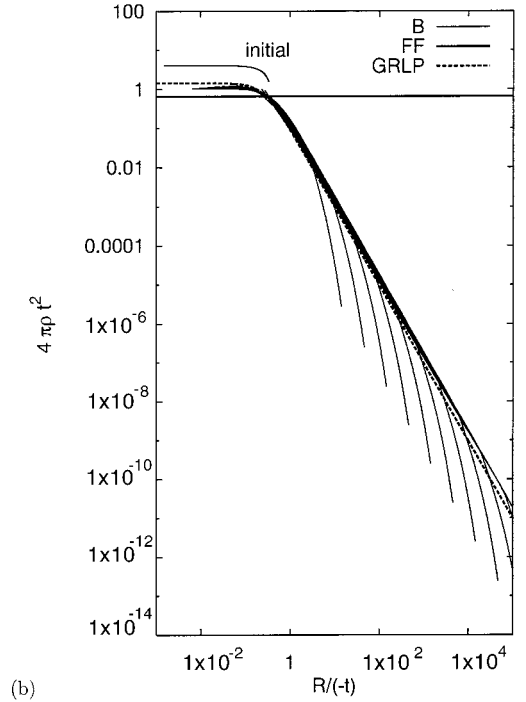
$$y = \frac{1}{3} \quad (2.51)$$

and

$$V_z = -C_k^{-2/3} (2D)^{-1/3(1+k)} z^{(1+3k)/3(1+k)}. \quad (2.52)$$



(a)



(b)

FIG. 3. Time evolution of the density profile for models (a) A and (b) B for $k=0.01$. The ordinate and abscissa are $4\pi\rho t^2$ and $R/(-t)$, respectively. For comparison, the FF and GRLP are also plotted.

For the FF, the big crunch occurs at $t=0$, i.e., the singularity occurs at the same time everywhere.

For $k \leq 0.036$, there exists a pure collapse solution. It tends to the Larson-Penston solution in Newton gravity in the limit $k \rightarrow 0$. Hereafter we call this solution the general relativistic Larson-Penston (GRLP) solution. For this solution, we have found that the value of the parameter D is

given by

$$D \approx 1.439 \quad (2.53)$$

for $k=0.01$. This coincides with the result of Ori and Piran [13,27,28].

We have another two analytic solutions. These solutions are general relativistic counterparts of Newtonian self-similar solutions, Hunter (a) and (b) [5]. We call these solutions GRHA and GRHB solutions, respectively. These similarity solutions are displayed in Figs. 1(a)–1(g).

The FF is the only solution which has the big crunch singularity. Unlike the FF, the solution of the black hole and repulsive types is regular at $t=0$, except for at $r=0$. It implies that the dimensionless physical quantities, such as M , S and η , are finite, i.e.,

$$M = M_\infty, \quad (2.54)$$

$$S = S_\infty, \quad (2.55)$$

$$\eta = \eta_\infty = \frac{M_\infty}{S_\infty^3}, \quad (2.56)$$

$$y = 1, \quad (2.57)$$

and

$$V_R = V_{R_\infty}, \quad (2.58)$$

at $z = \pm\infty$. The solution is black hole type if $V_{R_\infty} > 0$ and repulsive type if $V_{R_\infty} < 0$. It is found that the GRLP and GRHB are black hole type solutions while the GRHA is a repulsive type one. From the above equations, we find

$$\rho = \frac{\eta_\infty S_\infty^2}{8\pi R^2}, \quad (2.59)$$

at $t=0$. The velocity function V_z diverges as $z \rightarrow \infty$ as

$$V_z \approx -(2D)^{-k/(1+k)} \eta_\infty^{-(1-k)/(1+k)} S_\infty^{-2} z^{(1-k)/(1+k)}. \quad (2.60)$$

The number of oscillations of V_R , which coincides with the number of zeroes of $(y-1)$ in the domain $0 < z < \infty$, is 0, 0, 1 and 2 for the FF, GRLP, GRHA, and GRHB, respectively. The value of D we have obtained for self-similar solutions are summarized in Table I for $k=0.001$, 0.008, 0.01, and 0.03.

III. NUMERICAL EVIDENCE FOR CONVERGENCE TO GRLP

A. Numerical simulations

In order to see the generic feature of gravitational collapse, we have numerically simulated the spherical collapse of a perfect fluid. We have numerically solved the full Einstein equations (2.3)–(2.7) by the standard Misner-Sharp code without the self-similarity ansatz. The finite difference equations have been given by the staggered-leapfrog scheme.

The distribution of grid points has been not homogeneous but concentrated in the neighborhood of the center. The total number of the grid points has been 10000. See Harada [29] for details of the numerical code and references are therein.

For simplicity we display the results for time symmetric initial data. It should be noted that we have confirmed that the results do not change so much for several models in which initial data is not time symmetric. As a set of initial data, we have prepared both homogeneous and inhomogeneous balls of a perfect fluid which are momentarily static with vacuum external. For the inhomogeneous models, the density profile has been given by

$$\rho = \begin{cases} \rho_{c,i} \left[1 - \left(\frac{R}{R_{s,i}} \right)^2 \right], & 0 \leq R \leq R_{s,i}, \\ 0, & R_{s,i} < R. \end{cases} \quad (3.1)$$

Since we have confirmed that the results do not depend so much on the detailed form of the density profile, the above functional form is considered to represent a typical situation. The models which we have simulated are summarized in Table II, where \mathcal{M} is the Arnowitt-Deser-Misner (ADM) mass of the ball.

For $k=0.01$, we plot the time evolution of the density profile of models A and B in Figs. 2(a) and 2(b), respectively. We can see that model B collapses in a self-similar manner near the center as the collapse proceeds. In particular, the density profile around the center tends to $\rho \propto R^{-2}$ in an approach to the occurrence of singularity, which is characteristic to the self-similar solutions as we have seen. In order to see more clearly that the collapse approaches the self-similar solution, we plot in Figs. 3(a) and 3(b) the time evolution of the density profile of models A and B for $k=0.01$, respectively. The ordinate and abscissa are dimensionless quantities $4\pi\rho t^2$ and $R/(-t)$, respectively, where t is the proper time at the center and $t=0$ is chosen as the occurrence of singularity. For comparison, we also plot the FF and GRLP in these figures using the relations $4\pi\rho t^2 = (1/2)\eta z^{-2}$ and $R/(-t) = Sz$. It is found that model B approaches the GRLP while model A approaches the FF in an approach to the singularity. As seen in Figs. 1(b) and 1(e), $R/(-t) \approx 0.26$ and 0.28 at the sonic point for the FF and GRLP, respectively. Therefore, from Figs. 3(a) and 3(b), it is found that the approach to the FF and GRLP is not only for the subsonic region but also for the supersonic region.

Moreover, in order to see which self-similar solution the collapse approaches, we have calculated the quantity D which is defined by

$$D \equiv 4\pi\rho_c t^2, \quad (3.2)$$

where ρ_c is the central density. This definition is consistent with Eq. (2.41). Actually, we have determined the origin of t by requiring that the above defined D tends to be constant. The results for $k=0.001$, 0.008, 0.01, and 0.03 are plotted in Figs. 4(a)–4(d). Then, we have found that for $k=0.008$, 0.01, and 0.03 most models converge to the GRLP. Model A for $k=0.001$, 0.008, and 0.01 and model C for $k=0.001$ turn out to be trivial counterexamples against the convergence.

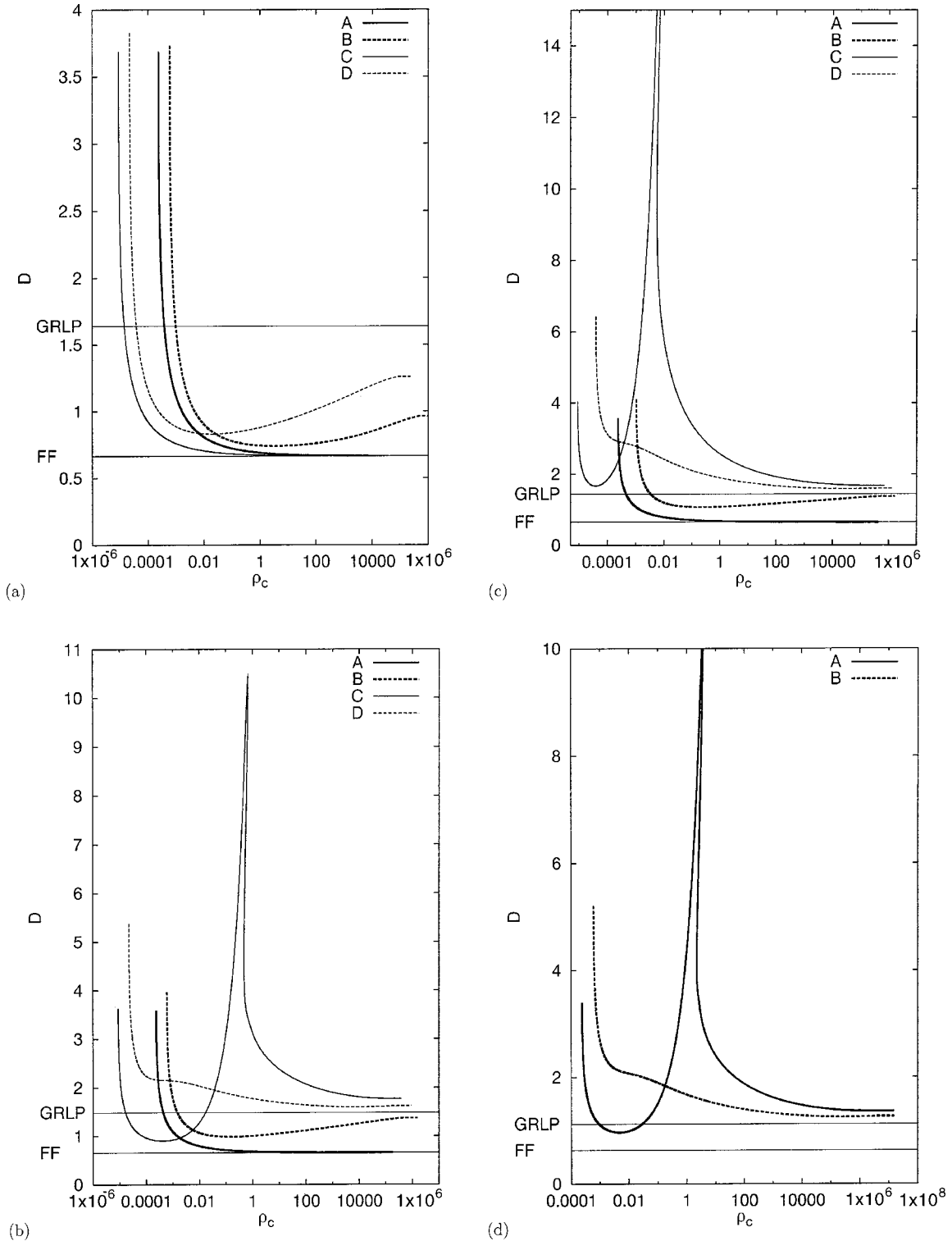


FIG. 4. $D = 4\pi\rho_c t^2$ for (a) $k = 0.001$, (b) $k = 0.008$, (c) $k = 0.01$, and (d) $k = 0.03$ are plotted. The abscissa is the central density ρ_c . The values of D for the FF ($D = 0.6653, 0.6561, 0.6535, \text{ and } 0.6284$) and for the GRLP ($D = 1.640, 1.480, 1.439, \text{ and } 1.119$) for $k = 0.001, 0.008, 0.01, \text{ and } 0.03$ are also denoted, respectively.

We will discuss them later. The results of numerical simulations are summarized in Table III. The resolution of our code has not been sufficient to show the convergence of models B and D to the GRLP for $k = 0.001$, although some tendency towards the GRLP has been observed. For dust collapse (k

$= 0$), we can easily find that the above defined D approaches $2/3$, using the Lamaitre-Tolman-Bondi solution. Therefore, from the continuity with respect to k , it is expected that the convergence to the GRLP becomes slower as k goes to zero. In fact, since the Newtonian approximation becomes good

TABLE III. Asymptotic behavior of the collapse models.

Models	$k=0.001$	0.008	0.01	0.03
A	FF	FF	FF	GRLP
B	GRLP?	GRLP	GRLP	GRLP
C	FF	GRLP	GRLP	(Dispersion)
D	GRLP?	GRLP	GRLP	(Dispersion)

for $k \ll 1$, it can be said that the convergence to the GRLP for $k \ll 1$ has been confirmed by Newtonian SPH simulations, by Tsuribe and Inutsuka [6]. Then, we conclude that the results of numerical simulations strongly suggest that generic spherical collapse converges to the GRLP in an approach to the singularity occurrence in both space and time.

B. Interpretation

As we have seen in Sec. III A, most collapse models approach the GRLP, though several models do not approach the GRLP. Here we interpret the results analytically.

First, we consider homogeneous models such as model A for $k=0.001, 0.008$, and 0.01 and model C for $k=0.001$. For an initially time symmetric homogeneous ball, the evolution of the central region is described by the closed Friedmann solution until the rarefaction wave propagates from the surface to the center. The line element of the homogeneous central region is written as

$$ds^2 = -dt^2 + a^2[d\chi^2 + \sin^2\chi(d\theta^2 + \sin^2\theta d\phi^2)]. \quad (3.3)$$

The initial value a_i of the scale factor a and the surface value χ_s of the comoving coordinate χ are written using the initial density ρ_i and the initial circumferential radius $R_{s,i}$ as

$$a_i^2 = \frac{3}{8\pi\rho_i}, \quad (3.4)$$

$$\chi_s = \text{Arc sin}\left(\frac{R_{s,i}}{a_i}\right). \quad (3.5)$$

Therefore, the central region of the initially time symmetric ball begins to contract for $k > -1/3$. We restrict our attention to $k > 0$. If the sound wave does not reach the center until the central Friedmann region collapses to the big crunch singularity, the central region approaches not the GRLP, but the FF. For $k \ll 1$, the central homogeneous part is well described by the closed Friedmann solution with dust, which has the parametrized representation as

$$a = a_i \frac{1 + \cos 2\theta}{2}, \quad (3.6)$$

$$t - t_i = a_i \left(\theta + \frac{1}{2} \sin 2\theta \right). \quad (3.7)$$

The big crunch occurs at $\theta = \pi/2$, i.e., $t - t_i = \pi a_i/2 = \sqrt{3}\pi/(32\rho_i)$. The trajectory of the rarefaction wave with the sound speed $c_s = \sqrt{k}$ which emanates from the surface at $t = t_i$ satisfies

$$a \frac{d\chi}{dt} = -c_s, \quad (3.8)$$

which can be integrated as

$$\chi = \chi_s - 2c_s\theta. \quad (3.9)$$

Therefore, the condition for the sound wave not to reach the center before the big crunch is given by

$$\frac{\chi_s}{c_s} > \pi. \quad (3.10)$$

Using the free-fall velocity v_{ff} defined as

$$v_{ff} \equiv \sqrt{\frac{2\mathcal{M}}{R_{s,i}}}, \quad (3.11)$$

we find the condition

$$\frac{c_s}{v_{ff}} < \frac{1}{\pi}, \quad (3.12)$$

or that the compactness $\mathcal{M}/R_{s,i}$ satisfies

$$\frac{\mathcal{M}}{R_{s,i}} > \frac{\pi^2}{2}k, \quad (3.13)$$

where we have used $k \ll 1$. Equation (3.13) can explain the results of the numerical simulations. Condition (3.12) completely agrees with that for Newton gravity derived by Tsuribe and Inutsuka [6], although the present situation can be highly relativistic. In particular, the present analysis is valid even for the evolution inside an apparent horizon. Although we have discussed the initially time symmetric case, it is easy to derive a similar condition for the collapse in which the central homogeneous region, which is not swept by the rarefaction wave, is described by the Friedmann solution, which may be not only the closed Friedmann solution but also the flat or open Friedmann solution. The result is the same as Eq. (3.13).

In general, we can enumerate the following trivial counterexamples against the convergence to the GRLP. If the central region can be initially described by the Friedmann solution, then the central region does not approach the GRLP, but the FF instead, if the big crunch occurs before the rarefaction wave reaches the center.

Moreover, it is clear that the *exact* self-similar solutions other than the GRLP do not approach the GRLP. There are another kind of counterexamples. We divide the initial data at $R = R_p$ into two regions: the central region and the surrounding region. If the initial data in the central region is the same as those of the exact self-similar solutions other than the GRLP, and R_p is so large that the sound wave cannot

reach the center until the central singularity forms, the collapse in the neighborhood of the center is described not by the GRLP but by the self-similar solution initially prepared in the central region.

Finally, it should be noted that there exists another type of counterexamples, which can be obtained by the *exact fine-tuning* of parameters which characterize the initial data. We will discuss this type of counterexamples in Sec. IV.

Anyway, it is clear that a set of the above trivial counterexamples occupies only zero-measure in the space of the whole of regular initial data.

IV. MODE ANALYSIS

As we have seen in Sec. III, the results of numerical simulations suggest that only the GRLP has an attractive nature. In order to confirm this, we examine the behavior of modes in linear perturbations of the self-similar solutions.

A. Perturbation equations

We consider the spherically symmetric perturbation around the fixed self-similar solution. We attach the suffix $_0$ for the background solution. Using the rescaling freedom, we set the arbitrary functions a_σ and a_ω to the background value, i.e.,

$$a_\sigma = a_{\sigma 0} = (2D)^{2k/(1+k)}, \quad (4.1)$$

$$a_\omega = a_{\omega 0} = 1. \quad (4.2)$$

We define the perturbation quantities as

$$M = M_0(z)[1 + \epsilon M_1(\tau, z) + O(\epsilon^2)], \quad (4.3)$$

$$S = S_0(z)[1 + \epsilon S_1(\tau, z) + O(\epsilon^2)], \quad (4.4)$$

$$\eta = \eta_0(z)[1 + \epsilon \eta_1(\tau, z) + O(\epsilon^2)], \quad (4.5)$$

$$y = y_0(z)[1 + \epsilon y_1(\tau, z) + O(\epsilon^2)], \quad (4.6)$$

where ϵ is a small parameter which controls the expansion. Then we find the equations for perturbations up to linear order of ϵ as

$$M'_1 = -\frac{k}{1+k} \frac{y_1}{y} - \frac{1}{1+k} (\dot{M}_1 + ky^{-1} \dot{S}_1), \quad (4.7)$$

$$S'_1 = \frac{1}{1+k} yy_1 - \frac{1}{1+k} y(\dot{M}_1 + ky^{-1} \dot{S}_1), \quad (4.8)$$

$$\begin{aligned} & \frac{1}{2}(1+k)^2 y \eta^{-(1-k)/(1+k)} S^{-4} (M_1 - S_1) \\ &= V_z^2 \left[(1-y)^2 \left(\frac{k}{1+k} \eta_1 + S_1 \right) \right. \\ & \quad \left. - (1+k)(1-y)(\dot{S}_1 + S'_1) \right] \\ & \quad - \left[(k+y)^2 \left(\frac{1}{1+k} \eta_1 + 3S_1 \right) + (1+k)(k+y)S'_1 \right], \end{aligned} \quad (4.9)$$

$$y_1 = M_1 - \eta_1 - 3S_1, \quad (4.10)$$

where we have omitted the suffix $_0$ for simplicity.

Assuming the time dependence of the perturbative quantities $Q_1(\tau, z) = e^{\lambda \tau} Q_1(z)$, we find the following set of simultaneous equations:

$$M'_1 = -\frac{k}{1+k} \frac{y_1}{y} - \frac{\lambda}{1+k} (M_1 + ky^{-1} S_1), \quad (4.11)$$

$$S'_1 = \frac{1}{1+k} yy_1 - \frac{\lambda}{1+k} y(M_1 + ky^{-1} S_1), \quad (4.12)$$

$$\begin{aligned} (V_z^2 - k)(1-y)(k+y)y_1 = & \left[kV_z^2(1-y)^2 - (k+y)^2 - \frac{1}{2}(1+k)^3 \eta^{-(1-k)/(1+k)} y S^{-4} + (1+k)y(V_z^2(1-y) + (k+y))\lambda \right] M_1 \\ & + \left[(1-2k)V_z^2(1-y)^2 - 3k(k+y)^2 + \frac{1}{2}(1+k)^3 \eta^{-(1-k)/(1+k)} y S^{-4} \right. \\ & \left. - (1+k)(V_z^2(1-y) - k(k+y))\lambda \right] S_1. \end{aligned} \quad (4.13)$$

We can derive another dependent equation as

$$\begin{aligned} (V_z^2 - k)(1-y)(k+y)y'_1 = & \left[kV_z^2(1-y)((1-y)(\ln V_z^2)' - 2y(\ln y)') - 2(k+y)y(\ln y)' \right. \\ & \left. - \frac{1}{2}(1+k)^3 \eta^{-(1-k)/(1+k)} y S^{-4} \left(-\frac{1-k}{1+k} (\ln \eta)' + (\ln y)' - 4(\ln S)' \right) \right. \\ & \left. + (1+k)y((V_z^2(1-2y) + (k+2y))(\ln y)' + V_z^2(1-y)(\ln V_z^2)') \lambda \right] M_1 \end{aligned}$$

$$\begin{aligned}
 & + \left[kV_z^2(1-y)^2 - (k+y)^2 - \frac{1}{2}(1+k)^3 \eta^{- (1-k)/(1+k)} y S^{-4} + (1+k)y(V_z^2(1-y) + (k+y))\lambda \right] M_1' \\
 & + \left[(1-2k)V_z^2(1-y)((1-y)(\ln V_z^2)' - 2y(\ln y)') - 6k(k+y)y(\ln y)' \right. \\
 & + \frac{1}{2}(1+k)^3 \eta^{- (1-k)/(1+k)} y S^{-4} \left(-\frac{1-k}{1+k}(\ln \eta)' + (\ln y)' - 4(\ln S)' \right) \\
 & \left. - (1+k)(V_z^2(1-y)(\ln V_z^2)' - (V_z^2+k)y(\ln y)')\lambda \right] S_1 \\
 & + \left[(1-2k)V_z^2(1-y)^2 - 3k(k+y)^2 + \frac{1}{2}(1+k)^3 \eta^{- (1-k)/(1+k)} y S^{-4} \right. \\
 & \left. - (1+k)(V_z^2(1-y) - k(k+y))\lambda \right] \\
 & \times S_1' - [V_z^2(1-y)(k+y)(\ln V_z^2)' + (V_z^2-k)(1-k-2y)y(\ln y)'] y_1, \tag{4.14}
 \end{aligned}$$

where $(\ln y)'$ and $(\ln V_z^2)'$ are given by

$$(\ln y)' = (\ln M)' - (\ln \eta)' - 3(\ln S)', \tag{4.15}$$

$$(\ln V_z^2)' = 2\frac{1-k}{1+k} - 2\frac{1-k}{1+k}(\ln \eta)' - 4(\ln S)'. \tag{4.16}$$

Then we examine boundary conditions which the perturbation quantities should satisfy at the boundaries. First, we consider the regular center $z = +0$. At the regular center, the definition of y implies that the perturbation of y must vanish at $z = +0$, since the background solution already satisfies the boundary condition in full order. Then we obtain

$$y_1 = 0 \tag{4.17}$$

at $z = +0$. From Eq. (4.13), it implies the following condition:

$$M_1 + 3kS_1 = 0. \tag{4.18}$$

Then, the perturbation solutions, which are regular at the center for fixed λ , are parametrized by one parameter Δ . The boundary condition at $z = +0$ is written as

$$y_1 = 0, \tag{4.19}$$

$$M_1 = \frac{k}{1+k} \Delta, \tag{4.20}$$

$$S_1 = -\frac{1}{3(1+k)} \Delta, \tag{4.21}$$

where

$$\Delta \equiv \eta_1(0) = \frac{\delta \rho}{\rho}(t = -1, r = 0). \tag{4.22}$$

Δ only scales y_1 , M_1 , and S_1 because we are only considering the linear perturbations. Hence, we can set the parameter Δ as $\Delta = 1$ without loss of generality.

Next, we consider the sonic point $z = z_{\text{sp}}$. At the sonic point, we require that the density perturbation is regular. It implies that M_1 , S_1 , and y_1 must satisfy the condition that the right-hand side of Eq. (4.14) vanishes at the sonic point. Only for a discrete set of λ , there exists a solution of perturbation equations that is regular both at the regular center and at the sonic point. Thus we can obtain eigenvalues λ and the associated eigenmodes.

B. Results of mode analysis

It is found that the system has a gauge mode with the eigenvalue λ given by

$$\lambda = \frac{1-k}{1+k}. \tag{4.23}$$

The mode functions are given by

$$M_1 = \frac{\Delta}{2} (\ln M)', \tag{4.24}$$

$$S_1 = \frac{\Delta}{2} (\ln S)', \tag{4.25}$$

$$y_1 = \frac{\Delta}{2} (\ln y)'. \tag{4.26}$$

This mode corresponds to the following gauge transformation:

$$(-t) \rightarrow (-t) - \epsilon \frac{\Delta}{2} (-t)^{2k/(1+k)}, \tag{4.27}$$

TABLE IV. Eigenvalues λ for repulsive modes of self-similar solutions.

	$k=0.001$	0.008	0.01	0.03
FF	None	None	None	None
GRLP	None	None	None	None
GRHA	9.39	8.88	8.75	7.62
GRHB	5.43	5.10	5.02	4.27
	5.62×10	4.90×10	4.71×10	3.30×10

$$r \rightarrow r \quad (4.28)$$

or, equivalently,

$$\tau \rightarrow \tau - \epsilon \frac{\Delta}{2} e^{(1-k)/(1+k)} \tau, \quad (4.29)$$

$$z \rightarrow z + \epsilon \frac{\Delta}{2} e^{(1-k)/(1+k)} \tau_z. \quad (4.30)$$

The eigenvalues of physical repulsive modes for $k = 0.001, 0.008, 0.01, \text{ and } 0.03$ are summarized in Table IV, where $\lambda \in \mathbf{R}$ is assumed. For the FF and GRLP, there exists no repulsive mode. On the other hand, the GRHA and GRHB have one and two repulsive modes, respectively. Therefore, it is found that only the FF and GRLP can describe the final stage of the central region of generic collapse. Together with the existence of the ‘‘kink’’ instability in the FF and the self-similar solutions which are not analytic at the sonic point [13,30], we conclude that the GRLP is the only self-similar solution that can be an attractor. For the GRHA, there exists only one repulsive mode. This solution corresponds to the critical solution in the black hole critical behavior. Only when one parameter p , which parametrizes initial data, is fine-tuned around the critical value p^* for the black hole formation, this solution has importance as a critical solution. The critical exponent γ , which appears in the scaling law of the formed black hole mass $M_{BH} \propto (p - p^*)^\gamma$, is given by the inverse of this repulsive mode. For $k = 0.01$, the eigenvalue we have obtained agrees well with Maison [22]. Since the GRHA solution has a repulsive mode, it is not relevant for the behavior of generic collapse. In particular, the final stage of the collapse can be described by the GRHA if the parameter is *exactly* fine-tuned, i.e., $p = p^*$. The GRHB has two repulsive modes. It is expected from the mode analyses in Newton gravity [7], that the solution with n oscillations has n repulsive modes. In order for the solution with n oscillations to be relevant, n parameters must be fine-tuned. If the fine-tuning is not exact, the perturbation grows into nonlinear regime. Then, it is expected that the collapse will approach to the GRLP or disperse away.

V. DISCUSSIONS

First, we discuss the validity of self-similarity hypothesis. The results of the numerical simulations and mode analysis strongly suggest that generic spherical collapse of a perfect fluid with small k converges to the GRLP in an approach to the singularity. This means that the GRLP is an attractor

solution. Moreover, in Sec. III B, we have discussed several counterexamples against the convergence to the GRLP. It is surprising that these counterexamples are exactly self-similar or at least asymptotically self-similar in the neighborhood of the center. It should be noted that non-flat Friedmann solution also approaches to the FF asymptotically in an approach to the big crunch. Therefore, we can conjecture that *any cloud of a perfect fluid collapses in a self-similar manner in an approach to the singularity.*

Next we discuss the implications of the convergence to the GRLP in the context of the cosmic censorship. The cosmic censorship conjecture states that a naked singularity does not form in the gravitational collapse which develops from generic initial data with matter fields which obey a physically reasonable equation of state. For spherical collapse, the convergence to the GRLP, which we have observed in this paper, means that a naked singularity forms in generic collapse for an equation of state $P = k\rho$ for $0 < k \lesssim 0.0105$, because the GRLP has a naked singularity for that range of k [13,27,28].

Here we should give the precise terminology of a naked singularity. In this article, we refer to a singularity that can be seen by some observer as a naked singularity. In contrast, a naked singularity that can be seen from infinity is called a globally naked singularity. Whether a naked singularity is globally naked is determined not only by the central region but also by the surrounding region. In fact, a naked singularity treated here can be globally naked through the matching of the central region with an appropriate surrounding region.

Now that we have the precise terminology, we can discuss the consistency of our results with previous works on the black hole critical behavior. At first sight, our results seem to be inconsistent with the formation of an apparent horizon observed in numerical simulations showing the black hole critical behavior. In fact, this is not the case. Since the convergence is only for the neighborhood of the center, we cannot say whether the formed naked singularity is locally naked or globally naked. Because the formation of an apparent horizon only implies the existence of an event horizon outside or coinciding with it, it does not exclude the formation of locally naked singularity at the center.

If the cosmic censorship is true, then there are three possibilities. One is that deviations from spherical symmetry may play a crucial role in the nakedness of the formed singularity. Although there has been no systematic study on the effect of violation of spherical symmetry in inhomogeneous gravitational collapse, Shapiro and Teukolsky [31] reported some numerical results that suggest the occurrence of naked singularity in the axisymmetric collapse of collisionless particles. In contrast, Iguchi *et al.* [32–34] and Nakao *et al.* [35] reported some kind of instability along the Cauchy horizon associated with a globally naked singularity. The second possibility is that the small value of k is not allowed for extremely high-density matter fields. However, it seems to be strange that the consistency of classical theory of gravity restricts the equation of state for high-density matter fields, which is determined by a collection of various microscopic physics. The third possibility is that the fluid description for high-density matter may be responsible.

Whether or not the cosmic censorship conjecture is true, the convergence to the GRLP strongly suggests that there can appear an extremely high-density or high-curvature region which can be seen by an observer. Even for such an “approximate” naked singularity, it has been shown that explosive radiation is emitted due to quantum effects [36–43]. Furthermore, in a practical sense, if the curvature scale reaches the Planck scale, it should be regarded as a singularity because it is considered beyond the scope of classical general relativity.

Self-similar solutions we have obtained here approach those in Newton gravity in the limit $k \rightarrow 0$. Therefore, the important consequence is that critical phenomena associated with the Hunter (a) Newtonian self-similar solution should be observed in the collapse of isothermal gas in Newton gravity. These critical phenomena will be very similar to the critical phenomena in the black hole formation in general relativity. Only one parameter p has to be fine-tuned closely to the critical value p^* . In particular, some order parameter \mathcal{A} follows the scaling law $\mathcal{A} \propto (p - p^*)^\gamma$ in the near critical regime, where γ is given by the inverse of the eigenvalue of the only one repulsive mode of the Hunter (a) solution. Unfortunately, the eigenvalue of the repulsive mode of the Hunter (a) solution has not been known yet. However, by extrapolating our results on the GRHA to the limit $k \rightarrow 0$, we can predict that the critical exponent γ is given by $\gamma \approx 0.11$. The candidate for the order parameter \mathcal{A} will be, for ex-

ample, the mass of the initially formed core, if we assume the realistic equation of state for dense gas.

VI. CONCLUSIONS

The results of the numerical simulations and mode analysis strongly suggest that the general relativistic Larson-Penston solution is an attractor solution of spherically symmetric gravitational collapse of a perfect fluid with an adiabatic equation of state $P = k\rho$ for $0 < k \leq 0.036$ in general relativity. Since a naked singularity forms in the general relativistic Larson-Penston solution for $0 < k \leq 0.0105$, the analysis in this paper means the violation of cosmic censorship in spherically symmetric case. This will be the strongest known counterexample against the cosmic censorship ever. This also provides strong evidence for the self-similarity hypothesis in general relativistic gravitational collapse.

ACKNOWLEDGMENTS

We are very grateful to B. J. Carr, H. Kodama, T. P. Singh, K. Nakao, T. Hanawa and S. Inutsuka for helpful discussions and comments. We would also like to thank K. Maeda for continuous encouragement. This work was partly supported by the Grant-in-Aid for Scientific Research (No. 05540) from the Japanese Ministry of Education, Science, Sports and Culture.

-
- [1] B. J. Carr, in *Proceedings of the Ninth Workshop on General Relativity and Gravitation*, 1999, edited by Y. Eriguchi *et al.* (Hiroshima, Japan), p. 425, gr-qc/0003009.
 - [2] M. V. Penston, *Mon. Not. R. Astron. Soc.* **144**, 425 (1969).
 - [3] R. B. Larson, *Mon. Not. R. Astron. Soc.* **145**, 271 (1969).
 - [4] F. H. Shu, *Astrophys. J.* **214**, 488 (1977).
 - [5] C. Hunter, *Astrophys. J.* **218**, 834 (1977).
 - [6] T. Tsuribe and S. Inutsuka, *Astrophys. J.* **526**, 307 (1999).
 - [7] T. Hanawa and K. Nakayama, *Astrophys. J.* **484**, 238 (1997).
 - [8] T. Hanawa and T. Matsumoto, *Publ. Astron. Soc. Jpn.* **52**, 241 (2000).
 - [9] T. Hanawa and T. Matsumoto, *Astrophys. J.* **521**, 703 (2000).
 - [10] B. J. Carr and S. W. Hawking, *Mon. Not. R. Astron. Soc.* **168**, 399 (1974).
 - [11] G. V. Bicknell and R. N. Henriksen, *Astrophys. J.* **219**, 1043 (1978).
 - [12] G. V. Bicknell and R. N. Henriksen, *Astrophys. J.* **225**, 237 (1978).
 - [13] A. Ori and T. Piran, *Phys. Rev. D* **42**, 1068 (1990).
 - [14] M. W. Choptuik, *Phys. Rev. Lett.* **70**, 9 (1993).
 - [15] C. R. Evans and J. S. Coleman, *Phys. Rev. Lett.* **72**, 1782 (1994).
 - [16] M. Goliath, U. Nilsson, and C. Ugglä, *Class. Quantum Grav.* **15**, 167 (1998).
 - [17] M. Goliath, U. Nilsson, and C. Ugglä, *Class. Quantum Grav.* **15**, 2841 (1998).
 - [18] B. J. Carr and A. A. Coley, *Class. Quantum Grav.* **16**, R31 (1999).
 - [19] B. J. Carr, *Phys. Rev. D* **62**, 044022 (2000).
 - [20] B. J. Carr and A. A. Colley, *Phys. Rev. D* **62**, 044023 (2000).
 - [21] T. Koike, T. Hara, and S. Adachi, *Phys. Rev. Lett.* **74**, 5170 (1995).
 - [22] D. Maison, *Phys. Lett. B* **366**, 82 (1996).
 - [23] R. Penrose, *Riv. Nuovo Cimento* **1**, 252 (1969).
 - [24] R. Penrose, in *General Relativity, An Einstein Centenary Survey*, edited by S.W. Hawking and W. Israel (Cambridge University Press, Cambridge, UK, 1979), p. 581.
 - [25] D. M. Eardley and L. Smarr, *Phys. Rev. D* **19**, 2239 (1979).
 - [26] D. Christodoulou, *Commun. Math. Phys.* **93**, 171 (1984).
 - [27] A. Ori and T. Piran, *Phys. Rev. Lett.* **59**, 2137 (1987).
 - [28] A. Ori and T. Piran, *Gen. Relativ. Gravit.* **20**, 7 (1988).
 - [29] T. Harada, *Phys. Rev. D* **58**, 104015 (1998).
 - [30] A. Ori and T. Piran, *Mon. Not. R. Astron. Soc.* **234**, 821 (1988).
 - [31] S. L. Shapiro and S. A. Teukolsky, *Phys. Rev. Lett.* **66**, 994 (1991).
 - [32] H. Iguchi, K. Nakao, and T. Harada, *Phys. Rev. D* **57**, 7262 (1998).
 - [33] H. Iguchi, T. Harada, and K. Nakao, *Prog. Theor. Phys.* **101**, 1235 (1999).
 - [34] H. Iguchi, T. Harada, and K. Nakao, *Prog. Theor. Phys.* **103**, 53 (2000).
 - [35] K. Nakao, H. Iguchi, and T. Harada, *Phys. Rev. D* (to be published), OCU-PHYS-176, OU-TAP 139, WU-AP/105/00, gr-qc/0006057.
 - [36] S. Barve, T. P. Singh, C. Vaz, and L. Witten, *Nucl. Phys.* **B532**, 361 (1998).

- [37] S. Barve, T. P. Singh, C. Vaz, and L. Witten, *Phys. Rev. D* **58**, 104018 (1998).
- [38] C. Vaz and L. Witten, *Phys. Lett. B* **442**, 90 (1998).
- [39] T. Harada, H. Iguchi, and K. Nakao, *Phys. Rev. D* **61**, 101502(R) (2000).
- [40] T. Harada, H. Iguchi, and K. Nakao, *Phys. Rev. D* **62**, 084037 (2000).
- [41] T. Harada, H. Iguchi, T. P. Singh, T. Tanaka, K. Nakao, and C. Vaz, OCU-PHYS-178, WU-AP/115/00, YITP-00-56, gr-qc/0010101.
- [42] T. Tanaka and T. P. Singh, YITP-00-57, gr-qc/0010110.
- [43] H. Iguchi and T. Harada, submitted to *Class. Quantum Grav.*, WU-AP/121/01.